Vol 2 (2) (2021)

Measurement, Control, and Automation

Website: https:// mca-journal.org

ISSN 1859-0551

Modeling of Axial Flux Permanent Magnet Motors by a Finite Element Approach-Application to In-wheel Motorcycles

Xây dựng mô hình động cơ nam châm vĩnh cửu từ thông hướng trục bằng phương pháp phần tử hữu hạn- Ứng dụng cho xe máy điện

Bùi Minh Định[1] , Đặng Quốc Vương[1] and Nguyễn Huy Phương[1]

[1]Khoa Điện, Trường Điện – Điện tử, Trường đại học Bách Khoa Hà Nội
E-mail: dinh.buiminh@hust.edu.vn

Abstract

Axial flux permanent magnet motors have been applied for many electric vehicles due to the high torque and power densities, compact sizes and multipolar disc-type structure. In this paper, the axial flux permanent magnet motor with the concentrated winding, and axial flux-segmental rotor is studied to apply for in-wheel motorcycles, where the proposed structure consists of permanent magnet segments and slotted stators. By this way, the amount of permanent magnets are reduced and the scale up power and torque are high. This means that it makes the assembly easier and reduce the cost compared to conventional motors (e.g. BLDC motors). Especially, for a multipolar disc-type structure, the axial flux permanent magnet motors is easy to scale up power for the next models. The detailed design and operation of the proposed machine are presented, and the performance is also evaluated for an in-wheel traction application. The target design is impore torque per volume about 5 or 10% in comparison with conventional design which has torque per volume TRV (kN.m/m^3) is from 45 to 50. This paper will provide a multi-module design of AFPM for in wheel motorcycles in express delivery (Viettel post) with optimal magnet embrace angle.

Keywords: Axial-flux permanent magnet motor; Disc-type rotor; Sector stator; Wheel hub motor; Central motor, End winding.

Tóm tắt

Động cơ nam châm vĩnh cửu từ thông hướng trục được áp dụng cho nhiều loại xe điện do mật độ mô-men xoắn cao, kích thước nhỏ gọn và cấu trúc kiểu đĩa đa cực. Trong bài báo này, động cơ nam châm vĩnh cửu từ thông hướng trục roto phân đoạn với cuộn dây tập trung được nghiên cứu để ứng dụng cho xe điện, trong đó cấu trúc đề xuất bao gồm các đoạn nam châm vĩnh cửu với cấu trúc dạng đĩa đa cực và rãnh stator. Với cách đề xuất như vậy, sẽ giảm được trọng lượng lượng của nam châm vĩnh cửu giảm và nâng cao được công suất và mô-men xoắn. Điều này có nghĩa rằng việc lắp ráp dễ dàng thuận tiện hơn và giảm chi phí so với động cơ thông thường (như động cơ BLDC). Đặc biệt, với cấu trúc dạng đĩa đa cực, động cơ nam châm vĩnh cửu từ thông hướng trục dễ dàng mở rộng và cải tiến quy mô công suất cho các mô hình tiếp theo. Thiết kế chi tiết và đặc tính làm việc của động cơ được phân tích và đánh giá trong nội dung chính của bài báo. Mục tiêu của thiết kế đạt được cải thiện 5% đến 10% chỉ số mật độ mô men trên thể thích, so với thiết kế hiện có là 65 đến 80 kNm/m^3. Bài báo sẽ mang đến một thiết kế dạng nhiều mô đung cho xe máy điện ứng dụng trong chuyển phát nhanh-Viettelpost

1. Introduction

The axial flux permanent magnet (AFPM) motors are widely applied in practice due to high torque and power densities, higher torque-to-weight ratio with less core materials, smaller size, planar and easily adjustable air-gap, lower noise and vibration [1]. The conventional design uses permanent magnet rotor discs that result in the complexity of assembling the rotating components. This paper introduces a modular design with stator and rotor sectors. In order to simplify the structure and reduce the manufacturing cost, the axial flux motor topologies has also been investigated in the stator or rotor in back to back assembly. The sector topology of concentrated winding axial flux machine is proposed. The rotor disc is made of iron lamination segments embedded permanent magnetic frame. Compared to the existing AFPM topologies [1]-[3], the proposed AFPM is simplified and easy to assemble. The amount of permanent magnetics is also reduced with its location secured in the stationary part. It is being considered for an in-wheel electric vehicle application because of its compactness and high torque and power densities in this research. The details on the operating principle, machine structure, and design of the proposed AFPM topology for a targeted benchmark are presented in this paper.

2. Inertial sizing computation of AFPM

Two rotor and stator topologies are proposed for the AFPM. The detailed structure of the proposed multi stator and rotor AFPM is presented in Figure 1.

The double-stator variants are more complex due to the two winding sections. On the other hand, they are very space-saving, because the rotor is used by both stators. This reduces the overall cost, since less material is needed for the permanent magnets. In addition, the utilization of the permanent magnets is higher, as they are exposed to a stator field on either side. In case of the double-rotor machines shown in Figure 1 (*right*), there is only one magnetic return path on one side. An analytical expression of the sizing equation for axial

Received: 12 September 2021; Accepted: 19 January 2022.

flux permanent magnet synchronous machines is given as [6]-[8]

$$P_R = \frac{m}{m1}\frac{\pi}{2} K_e K_i K_p K_l \, \eta B_g A_S \,(D_o^2 - D_i^2) L_e \qquad (1)$$

where P_R, m, m_1, K_e, K_i, K_p, K_l, η are the real power, number phase, stator phase, back EMF factor, current factor, pole factor, stack length factor and efficiency, respectively. In addition, the parameters D_i and D_o are the inner and outer diameters (m), L_e is the length of core (m) and B_g is the airgap length and A_S is the pole area.

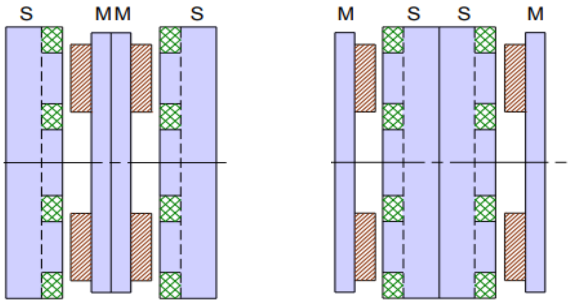

a. Inner rotor SMMS b. Outer rotor MSSM

Figure 1. Variants of axial-flux permanent magnet motor

Figure 1 provides two variants of axial-flux permanent magnet motor with inner mover or rotor (SMMS) and outer rotor MSSM. In this study, the electromagnetic performances are the same only the thermal distribution of two variants is changed due to the cooling system for them.

The effective stack or axial length of the AFPM depends on the of rotor and stator axial lengths written as

$$L_e = L_s + 2L_r + 2g \qquad (2)$$

where L_s is the length of Stator (m), g is the airgap length and L_r is length of rotor.

The axial length of the rotor can be obtained from the axial length of rotor core and the length of the permanent magnets. The geometry parameters of the stator and rotor can be calculated via the process of computation shown in Figure 2. An analytical model is presented by many calculation steps to define basic parameters. Based on the torque volume density (TVR) from 45kN/m^3 to 50 kNm/m^3 [4], [5], if we assume rotor diameter equal to rotor length, the rotor diameter D and length L sizes of the PM is defined [9], [10]

$$\mathrm{T} = \frac{\pi}{4}.\mathrm{D}^2.\mathrm{L_S}.\mathrm{TRV}, \qquad (3)$$

where T is the electromagnetic torque (N.m), D is the outer diameter (m), L_S is the length of core (m) and TVR is the torque and volume ratio (kNm/m^3).

In general, the design process of Permanent Magnet assisted Synchronous Reluctance Motor (PMa-SynRM) is similar to that of the induction motor. The main parameters (such as outer diameter, rotor diameter, motor length, stator slot, airgap length) are defined by considering some practical factors with desired input requirements.

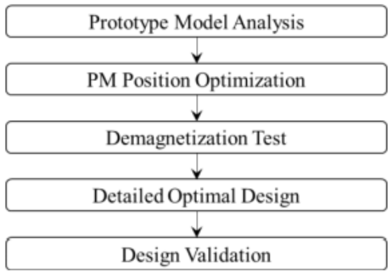

Figure 2. Process of computation.

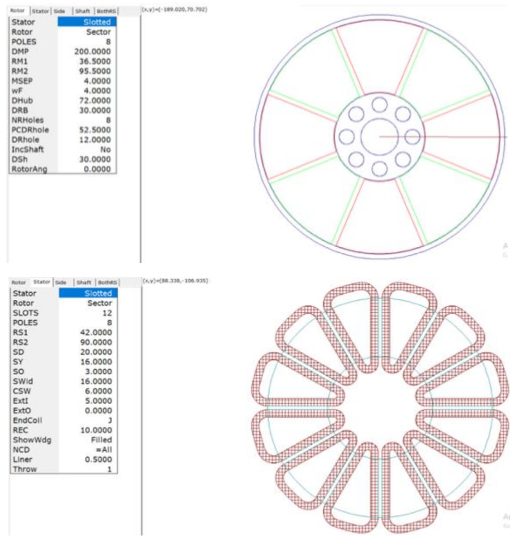

Figure 3. Structure of stator (*top*) and rotor (*bottom*).

The proposed machine is designed for an in-wheel electric vehicle application with high specific torque with the same design specifications. The design parameters and output specifications for the AFPM-SRM are given in Tables (2, 3 and 4). The main part of the process is to design the rotor configuration which is embedded permanent magnet.

Table 1. Design parameters.

Parameters Value	**Parameter Values**
Power Output	3000 Watts
Operational Voltage	72 Volts
Efficiency	0.95
Phase	3

Table 2. Stator specification.

Parameters	**Value**
Number of Pole	8
Number of Slot	12
Circuit Type	Y3
Outer Diameter	166 mm
Inner Diameter	80 mm
Length	45 mm

Table 3. Stator winding.

Parameters	**Value**

Parallel Branches	4
Number of Coils	48
Number of Strands	4
Wire Wrap	0.2
Wire Size	1.151 mm^2
Conductor Type	Copper

For the proposed tooth wound configuration, the magnetic flux will flow through one stator tooth to the next one via the rotor segments, but it will not flow through the stator back. Therefore, the segmental stator poles can be designed with the improved filling factor and the slot design for this tooth wound topology. Moreover, embedding the stator segments in non-magnetic support will also reduce the leakage flux and improve the percentage of active materials used for torque production. The design optimization and performance analysis of the tooth wound AFPM will be presented in this paper. The machine is designed to operate as a synchronous machine.

Table 4. Rotor specification.

Parameters	**Value**
Number of Pole	8
Outer Diameter	166 mm
Inner Diameter	80 mm
Length	10 mm
Magnet Embrace	135^0-165^0
Material Type Steel	250A-35

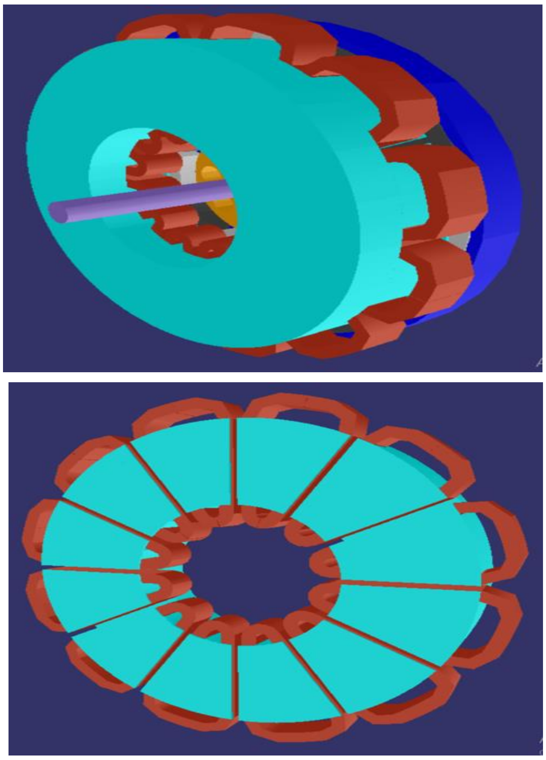

Figure 4. Detailed 3D structure of the proposed AFPM.

3. Simulation results

The AFPM is evaluated under the design constraints presented in Table 1. The AFPM is designed and simulated using 3-D finite element method (FEM) tool to compare their performances under the same simulation environment pointed out in Figure 4. Dynamic simulations have been performed at 1500 rpm to evaluate their performance at base speed and compare machines' torque capability under the same RMS phase current and current density. The proposed AFPM topology is excited with three-phase sinusoidal excitation The AFPM is simulated under current regulated unipolar excitation with each phase contributing for half of an electrical cycle. The dynamic torque profile for the designed AFPM is shown in Figure 5 for varying phase excitations.

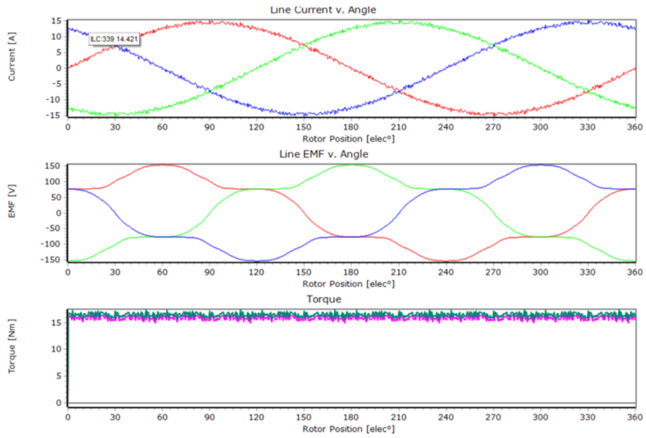

Figure 5. Phase Current, back EMF and torque of AFPM.

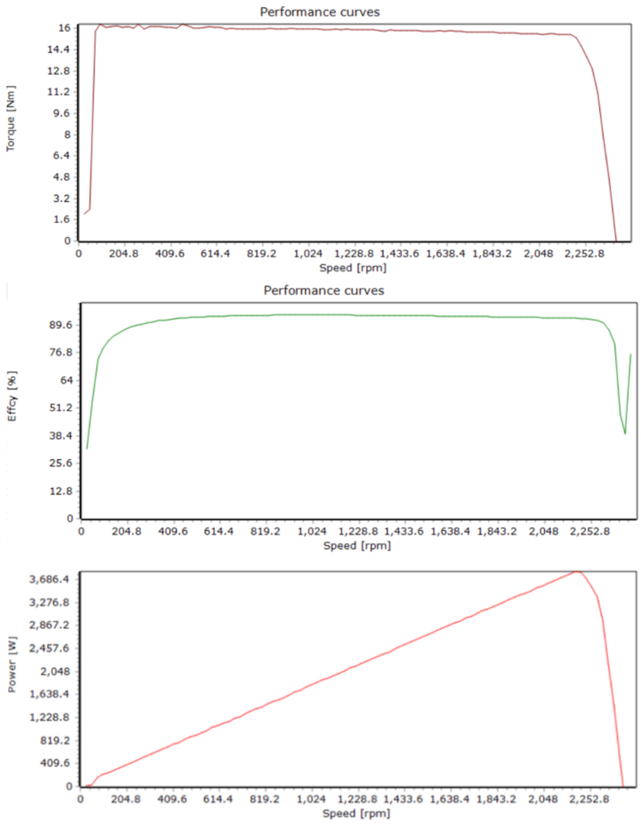

Figure 6. Distribution of the output torque (*top*), efficiency (*middle*) and power (*bottom*).

Figure 6 shows the simulated torque, power and efficiency and motor speed in peak torque mode with at maximum temperature of 110^0C in winding and 80^0C in a permanent magnet in worst case. Peak power is 3900W at 2200 r/min and constant torque of 16 N.m and efficiency of 89.6%. The proposed AFPM has a simplified and low-cost structure compared to the AFPMs, of which the multi-sector stator and rotor can provide much higher torque density and torque to weight ratio The performance comparison of the designed AFPM with an axial flux rotor PM machine will be presented.

Table 5. Detail results of AFPM at 2200 rpm.

Drive	Sine		Vs	72.0000	V	RPM	2200.0000	rpm
OpMode	Motoring		Tshaft	16.2148	Nm	Pshaft	3735.6154	W
Effcy	96.5730	%	TempRise	0.0000	°C	Pelec	3868.1793	W
ILpk	15.9997	A	ILmean	10.1859	A	ILrms	11.3136	A
VLpk	279.4642	V	VLmean	177.9123	V	VLrms	197.6112	V
IWpk	15.9997	A	IWmean	10.1859	A	IWrms	11.3136	A
VWpk	161.3488	V	VWmean	102.7177	V	VWrms	114.0909	V
Losses..								
WTotal	132.5639	W	WCu	32.3081	W	WFe	0.0000	W
WWF	96.8000	W	WFric	3.4558	W	WMagnet	0.0000	W
			WFeST	0.0000	W	WFeSY	0.0000	W

The electromagnetic results show that maximum efficiency can achieve with an optimal current phase angle of 45^0. The shaft torque can keep constant in a higher speed to 3000rpm at the peak value of the terminal voltage of 177V it exceeds supply voltage of 72 VDC. To improve electromagnetic performance, flux weakening should be applied and increase battery voltage by changing to the serial connection of cell module.

Table 6. The total weight of the iron and copper materials.

Weights..								
EWtMotor	8.2992	kg	WtStator	4.7467	kg	WtRotor	3.5525	kg
EMVol	0.0000	mm³						
WtFeR	1.8817	kg	WtFeRMP	1.8817	kg	WtFeRFP	0.0000	kg
WtMag	1.6708	kg	WtMagP	0.2088	kg			
WtFeSh	0.0000	kg	IncShaft	No		WtFrame	0.0000	kg
WtFeS	4.0381	kg	GWtFeS	4.0381	kg			
WtMB	0.1045	kg	WtCap	0.0330	kg			
WtCuS	0.7087	kg	WtCoil	0.0591	kg			

The average, power, and efficiency of the AFPM have been investigated at 1500 rpm with a current density of 6A/mm2 shown in Table 5. The maximum efficiency is of 96% with the optimal switching angle and current phase angle. The total weight of iron and copper material of moor is combined in Table 6. The torque per volume is calculated as below.

$$TRV = \frac{T\_avg}{\pi\frac{D^2}{4}L} = \frac{16\ N.m}{\pi\frac{0.166^2}{4}0.01} = 60.1\ (\mathrm{kN/m^3})$$

The analytical calculation model has been investigated magnet embrace angle from 135^0 to 165^0 considering minimum magnet cost and demagnetization due to over temperature.

4. Conclusion

The multi-sector topology for a dual rotor concentrated winding, axial flux machine is presented. Compared to the conventional BLDC motor, the proposed topology has higher torque and efficiency. The obtained results have been shown that the proposed AFPM topology can attain much higher torque density and torque-to-weight ratio compared to the BLDC motor under the same design constraints. The AFPM of the BLDC motor that is designed by the FEM design for the electric vehicle application. The AFPM motor of 3kW is designed with 12 stator slot numbers and 8 rotor poles. In addition, the motor's mechanical torque reached a value of 9.5 Nm at a speed of 1500 rpm with an input current of 60 A and input voltage of 72 V. Furthermore, the obtained motor efficiency is 94.49 %. The designed model can be a reference for the implementation and subsequent research. The obtained results can be validated by testing through the implementation.

Acknowledgement

The authors also gratefully acknowledge Quy Nhon University, created favorable conditions for the authors to use the copyright supported ANSYS software program to compute and simulate the practical problem in this research.

References

[1] Z. Q. Zhu, M. F. H. Khatab, H. Y. Li, and Y. Liu, “A novel axial flux magnetically geared machine for power split application”, Twelfth Int.Conf. Ecolo. Vehicles and Renewable Energies (EVER), 2017, pp. 1-8.

[2] Y. J. Cao, Y. K. Huang, and J. Long, “Research on axial magnetic force and rotor mechanical stress of an air-cored axial-flux permanent magnet machine based on 3D FEM,” Appl. Mech. Mater., vol. 105, pp. 160–163, Sep. 2012.

[3] Kahourzade, S.; Mahmoudi, A.; Hew Wooi Ping; Uddin, M.N., "A Comprehensive Review of Axial-Flux Permanent-Magnet Machines," Electrical and Computer Engineering, Canadian Journal of , vol.37, no.1, pp.19,33, winter 2014.

[4] Labak, A.; Kar, N.C., "Novel Approaches Towards Leakage Flux Reduction in Axial Flux Switched Reluctance Machines," Magnetics, IEEE Transactions on, vol.49, no.8, pp.4738-4741, Aug. 2013.

[5] Arihara, H.; Akatsu, K., "Basic Properties of an Axial-Type Switched Reluctance Motor," Industry Applications, IEEE Transactions on , vol.49, no.1, pp.59,65, Jan.-Feb. 2013.

[6] Labak, A.; Kar, N.C., "Designing and Prototyping a Novel Five-Phase Pancake-Shaped Axial-Flux SRM for Electric Vehicle Application Through Dynamic FEA Incorporating Flux-Tube Modeling," Industry Applications, IEEE Transactions on , vol.49, no.3, pp.1276,1288, MayJune 2013.

[7] Madhavan, R.; Fernandes, B.G., "Performance Improvement in the Axial Flux-Segmented Rotor-Switched Reluctance Motor," Energy Conversion, IEEE Transactions on, vol.29, no.3, pp.641-651, Sept. 2014.

[8] M. Johnson, M. C. Gardner, and H. A. Toliyat, "Design and analysis of an axial flux magnetically geared generator," IEEE Energy Conv. Congr. Expo. , 2015, pp. 6511-6518.

[9] Li Hao; Mingyao Lin; Da Xu; Xinghe Fu; Wei Zhang, "Static Characteristics of a Novel Axial Field Flux-Switching Permanent Magnet Motor with Three Stator Structures," IEEE Transactions on Magnetics, vol.50, no.1, pp.1,4, Jan. 2014.

[10] Zulu, A.; Mecrow, B.C.; Armstrong, M., "A Wound-Field Three-Phase Flux-Switching Synchronous Motor With All Excitation Sources on the Stator," Industry Applications, IEEE Transactions on , vol.46, no.6, pp.2363-2371, Nov.-Dec. 2010.